PID controller design with an H_∞ criterion

Sangjin Han * **Lee H. Keel** ** **Shankar P. Bhattacharyya** *

* *Department of Electrical and Computer Engineering, Texas A&M University, College Station, TX, 77840 USA (e-mail: sangjin.han,spb@tamu.edu).*
** *Department of Electrical and Computer Engineering, Tennessee State University, Nashville, TN, 37209 USA (e-mail: keel@gauss.tsuniv.edu).*

Abstract: This paper deals with the design of Proportional-Integral (PI) and Proportional-Integral-Derivative (PID) controllers. The main result is a constructive determination of the set S_γ of stabilizing PI and PID controllers achieving an H_∞ norm bound of γ on the error transfer function. This result utilizes the computation of the complete stabilizing set S recently obtained. We also point out connections between this H_∞ design and Gain and Phase Margin designs. Illustrative examples are presented.

Keywords: PID, stabilizing set, H_∞ norm, gain and phase margin, Nyquist plot

1. INTRODUCTION AND BACKGROUND

In servomechanisms the tracking error needs to be small for the class of reference signals and disturbance signals encountered. For step references and disturbances the integral controller yields zero steady state error provided the closed loop is stable. Integral control is usually implemented as a PI or PID controller in practice. In this paper we consider the additional design criterion of an H_∞ norm specification on the error transfer function and show that the complete set of PI and PID controllers satisfying H_∞ norm specification can be constructively determined.

In the next section we develop a relationship between H_∞ norm specification on the error transfer function and guaranteed classical gain and phase margins. Following this we present our constructive calculation of S_γ for PI or PID controller sets satisfying the given H_∞ norm specification of γ.

In Emami and Watkins (2009), the 2D regions of stabilizing PID controllers achieving the H_∞ norm bound of γ on the sensitivity and complementary sensitivity functions with weightings were found by using Neimark's D-decomposition. The difference is that our approach explicitly uses the *stabilizing set* S, and thus can determine the limits of achievable performance.

Similar approach was adopted by Tantaris et al. (2006) for first order controllers and in this case the stability region was computed a priori. Krajewski and Viaro (2012) showed that at a fixed frequency (and for a fixed k_d, the derivative gain) the L_2 norm of the error transfer function being equal to γ was represented by an ellipse in (k_p, k_i) space where k_p was the proportional gain and k_i was the integral gain.

An H_∞ optimal PID design using a frequency loop-shaping approach was reported in Tsakalis and Dash (2013); Ashfaque and Tsakalis (2012). PID gains were chosen by an optimization problem with a desired open loop transfer function. All PID gains were assumed to be positive in order for the constraint to be a convex set. However, the stabilizing set is not convex in general. See, for instance, Example 2.2 in Bhattacharyya et al. (2009).

The computation of all PID stabilizing controllers, the stabilizing set, and extensions were developed in Bhattacharyya et al. (2009). In Díaz-Rodríguez and Bhattacharyya (2016) the subset of the stabilizing set achieving prescribed gain and phase margin specifications were found.

2. H_∞ CONTROL AND STABILITY MARGINS

Consider the unity feedback system (see Fig. 1)

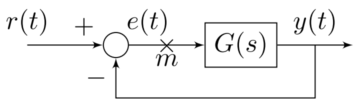

Fig. 1. Unity feedback control loop.

with the error transfer function

$$\frac{e(s)}{r(s)} = \frac{1}{1+G(s)}. \tag{1}$$

Suppose that $G(s)$ includes a controller designed to make the H_∞ norm of (1) less than γ, a prescribed real positive number. Then

$$\frac{1}{|1+G(j\omega)|} < \gamma, \qquad \text{for all } \omega \geq 0 \tag{2}$$

and (2) is equivalent to

$$|1+G(j\omega)| > \frac{1}{\gamma}, \qquad \text{for all } \omega \in [0,\infty). \tag{3}$$

We will now establish that (3) implies guaranteed gain and phase margins at the loop breaking point 'm' in Fig. 1.

Remark 1. Let γ^* denote the infimum value of γ satisfying (3). When $G(s)$ is strictly proper, $\gamma^* \geq 1$. When $G(s)$ is proper, $\gamma^* > 1/|1+G(j\infty)|$.

Case 1: $\gamma > 1$

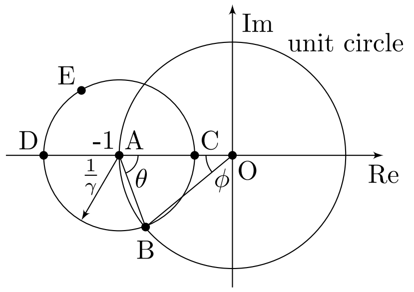

Fig. 2. $\gamma > 1$

The condition (3) implies that the Nyquist plot $G(j\omega)$ stays out of the circle CEDB centered at $-1 + j0$ and of radius $1/\gamma$. In Fig. 2, we have the limiting case in which $G(j\omega)$ passes through B, the phase margin is ϕ and

$$G(j\omega) = \overrightarrow{\mathrm{OB}}, \ -1 + j0 = \overrightarrow{\mathrm{OA}}, \ 1 + G(j\omega) = \overrightarrow{\mathrm{AB}}.$$

Since $\overrightarrow{\mathrm{OA}} + \overrightarrow{\mathrm{AB}} = \overrightarrow{\mathrm{OB}}$ and $\overrightarrow{\mathrm{OAB}}$ is an isosceles triangle,

$$-1 + j0 + \frac{1}{\gamma}e^{-j\theta} = -1e^{j\phi} \text{ and } 2\theta + \phi = \pi. \tag{4}$$

From (4),

$$-1 + \frac{1}{\gamma}\sin\left(\frac{\phi}{2}\right) = -\cos\phi \tag{5}$$

$$\sin\phi = \frac{1}{\gamma}\cos\left(\frac{\phi}{2}\right). \tag{6}$$

From (6),

$$\phi = 2\sin^{-1}\left(\frac{1}{2\gamma}\right) \tag{7}$$

which is the guaranteed minimum phase margin for the H_∞ controller with the norm less than γ.

The guaranteed gain margin is the interval:

$$\left[\frac{1}{\mathrm{OD}}, \frac{1}{\mathrm{OC}}\right] = \left[\frac{\gamma}{\gamma+1}, \frac{\gamma}{\gamma-1}\right]. \tag{8}$$

Case 2: $\gamma = 1$

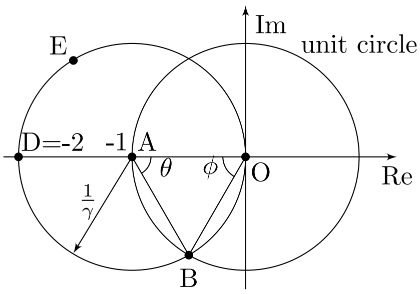

Fig. 3. $\gamma = 1$

In this case, Fig. 2 is replaced by Fig. 3. It is easy to see that the guaranteed phase margin is $\phi = \pi/3$ and the guaranteed gain margin is $\left[\frac{1}{2}, \infty\right]$. These also follow from formulas (7) and (8) evaluated at $\gamma = 1$.

Case 3: $\gamma < 1$
The geometry corresponding to this case is shown in Fig. 4 below.

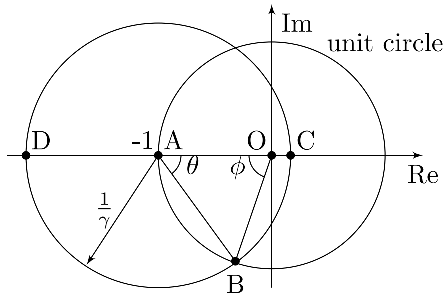

Fig. 4. $\gamma < 1$

In this case, it also follows that the guaranteed phase margin is

$$\phi = 2\sin^{-1}\left(\frac{1}{2\gamma}\right) \tag{9}$$

and the guaranteed gain margin is

$$\left[\frac{1}{\mathrm{OD}}, \infty\right] = \left[\frac{\gamma}{1+\gamma}, \infty\right]. \tag{10}$$

Combining the above cases, we have the following result.

Theorem 1. Consider the unity feedback system in Fig. 1. If the H_∞ norm of the error transfer function is less than γ:

$$\left\|\frac{1}{1+G(s)}\right\|_\infty < \gamma, \tag{11}$$

then the guaranteed phase margin at the loop breaking point 'm' is:

$$\phi = 2\sin^{-1}\left(\frac{1}{2\gamma}\right) \tag{12}$$

The guaranteed gain margin is:

$$g_m = \begin{cases} \left[\frac{\gamma}{\gamma+1}, \frac{\gamma}{\gamma-1}\right], & \text{for } \gamma > 1 \\ \left[\frac{\gamma}{\gamma+1}, \infty\right], & \text{for } \gamma \leq 1 \end{cases} \tag{13}$$

3. PROBLEM FORMULATION

Consider now the control system in Fig. 5.

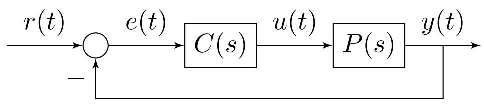

Fig. 5. Unity feedback control loop.

$r(t)$ is the reference signal, $e(t)$ is the error signal, $u(t)$ is the input signal (to the plant), $y(t)$ is the output signal, $P(s)$ is the plant transfer function and $C(s)$ is the controller transfer function which we will consider to be either PI or PID.

The problem to be solved in this paper is: find the set S_γ of all stabilizing PI or PID controllers satisfying

$$\left\|\frac{1}{1+P(s)C(s)}\right\|_\infty < \gamma. \tag{14}$$

4. MAIN RESULTS

In this section we develop the computation of S_γ for PI and PID controllers. Note that (14) is equivalent to

$$|1 + P(j\omega)C(j\omega)| > \frac{1}{\gamma}, \quad \forall\, \omega \in [0, \infty). \tag{15}$$

4.1 Computation of S_γ for PI controllers

PI controllers have the form:

$$C(s) = k_p + \frac{k_i}{s}. \tag{16}$$

Write

$$P(j\omega) = P_r(\omega) + j\omega P_i(\omega), \tag{17}$$

$$C(j\omega) = k_p - j\frac{k_i}{\omega}. \tag{18}$$

Substituting (17) and (18) in (15) we get

$$|1 + \underbrace{k_p P_r(\omega) + k_i P_i(\omega)}_{L_0(\omega)} + j\underbrace{(\omega k_p P_i(\omega) - \frac{k_i}{\omega} P_r(\omega))}_{L_1(\omega)}| > \frac{1}{\gamma} \tag{19}$$

which can be rewritten as

$$(1 + L_0(\omega))^2 + L_1^2(\omega) > \frac{1}{\gamma^2} \tag{20}$$

$$\begin{bmatrix} P_r(\omega) & P_i(\omega) \\ \omega P_i(\omega) & -\frac{P_r(\omega)}{\omega} \end{bmatrix} \begin{bmatrix} k_p \\ k_i \end{bmatrix} = \begin{bmatrix} L_0(\omega) \\ L_1(\omega) \end{bmatrix}. \tag{21}$$

(21) has a unique solution if

$$|P(j\omega)| \neq 0, \tag{22}$$

that is the plant has no $j\omega$ axis zeros.

Assuming (22), (21) can be solved:

$$\begin{bmatrix} k_p \\ k_i \end{bmatrix} = \underbrace{\frac{1}{|P(j\omega)|^2} \begin{bmatrix} P_r(\omega) & \omega P_i(\omega) \\ -\omega^2 P_i(\omega) & -\omega P_r(\omega) \end{bmatrix}}_{T(\omega)} \begin{bmatrix} L_0(\omega) \\ L_1(\omega) \end{bmatrix} \tag{23}$$

(20) represents the outside of a circle C_γ of radius $\frac{1}{\gamma}$ in the (L_0, L_1) plane centered at $(-1, 0)$:

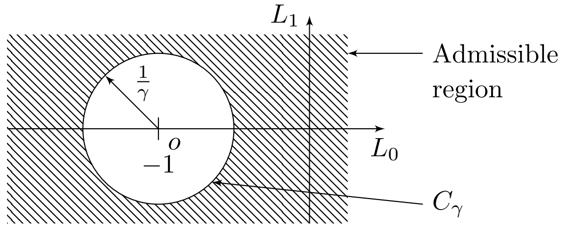

Fig. 6. The C_γ circle.

Let $E_\gamma(\omega)$ denote the mapping through (23) of the circle C_γ:

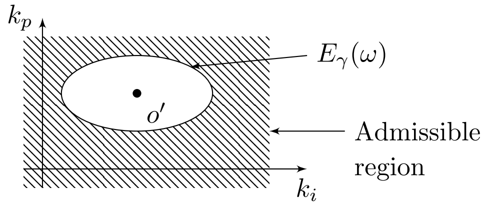

Fig. 7. The $E_\gamma(\omega)$ ellipse.

Lemma 1. Condition (15) at a fixed ω is equivalent to k_p, k_i lying in the complement of the interior of the axis parallel ellipse $E_\gamma(\omega)$ with center o' at $(\frac{-\omega^2 P_i(\omega)}{|P(j\omega)|^2}, \frac{-P_r(\omega)}{|P(j\omega)|^2})$, principal axes $\frac{2}{\gamma|P(j\omega)|}$, $\frac{2\omega}{\gamma|P(j\omega)|}$.

Proof. For each $\omega \geq 0$, (19) is

$$\left|1 + (P_r(j\omega) + j\omega P_i(j\omega))(k_p - j\frac{k_i}{\omega})\right| > \frac{1}{\gamma}$$

$$\Leftrightarrow (1 + P_r(j\omega)k_p + P_i(j\omega)k_i)^2 + \left(\omega P_i(j\omega)k_p - P_r(j\omega)\frac{k_i}{\omega}\right)^2 > \frac{1}{\gamma^2}. \tag{24}$$

After some algebra we obtain

$$\frac{(k_i - c_1)^2}{a^2} + \frac{(k_p - c_2)^2}{b^2} > 1 \tag{25}$$

where

$$c_1 = \frac{-\omega^2 P_i(\omega)}{|P(j\omega)|^2}, \; c_2 = \frac{-P_r(\omega)}{|P(j\omega)|^2}, \quad a = \frac{\omega/\gamma}{|P(j\omega)|}, \; b = \frac{1/\gamma}{|P(j\omega)|}. \tag{26}$$

□

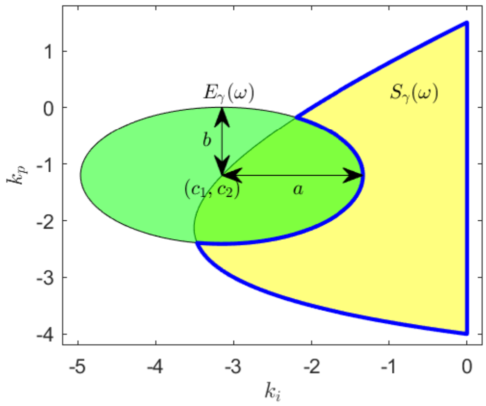

Fig. 8. $E_\gamma(\omega)$ and $S_\gamma(\omega)$.

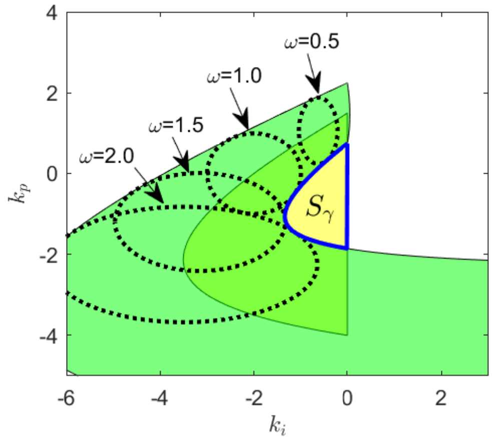

Fig. 9. S_γ.

For a fixed ω, let $S_\gamma(\omega)$ denote the intersection of the stabilizing set S with the exterior of the ellipse $E_\gamma(\omega)$ as shown in Fig. 8. In other words,

$$S_\gamma(\omega) = S \setminus E_\gamma(\omega) \ \ \forall\, \omega \in [0, \infty). \tag{27}$$

Since (15) must hold for all ω,

$$S_\gamma = \bigcap_{\omega=0}^{\infty} S_\gamma(\omega) \tag{28}$$

as shown in Fig. 9.

We state this result as the following theorem.

Theorem 2. In the unity feedback control loop, suppose that the plant $P(s)$ has no $j\omega$ axis zeros. All stabilizing PI controllers $C(s)$ satisfying the H_∞ norm bound of γ on the error transfer function is the set S_γ:

$$S_\gamma = \bigcap_{\omega=0}^{\infty} S_\gamma(\omega). \tag{29}$$

Proof. $S_\gamma(\omega)$ is the admissible set for each ω and the controller must satisfy the H_∞ norm for all frequencies. Hence we have the set S_γ by intersecting the admissible sets $S_\gamma(\omega)$ for all ω. □

Note that S can be determined using the concept of signature developed in Bhattacharyya et al. (2009). If $E_\gamma(\omega)$ is outside of S then $S_\gamma(\omega) = S$. If $S \subset E_\gamma(\omega)$ then S_γ is empty.

4.2 Computation of S_γ for PID controllers

PID controllers are of form:

$$C(s) = k_p + \frac{k_i}{s} + k_d s. \tag{30}$$

Substituting $s = j\omega$, we have

$$C(j\omega) = k_p - j\frac{1}{\omega}\left(k_i - \omega^2 k_d\right). \tag{31}$$

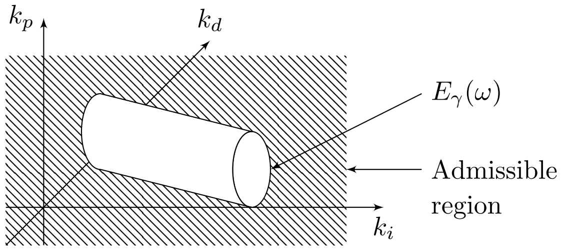

Fig. 10. The $E_\gamma(\omega)$ elliptic cylinder.

Replace k_i in (19) with $k_i' = k_i - \omega^2 k_d$. By analysis similar to the PI case, it is easy to show that (15) implies that the controller parameters k_p, k_i, k_d must lie in the exterior of $E_\gamma(\omega)$ described by:

$$\frac{\left(k_i - \omega^2 k_d - c_1\right)^2}{a^2} + \frac{\left(k_p - c_2\right)^2}{b^2} > 1 \tag{32}$$

which is an elliptic cylinder with the center lying on the line

$$\begin{cases} k_i - \omega^2 k_d = \frac{-\omega^2 P_i(\omega)}{|P(j\omega)|^2}, \\ k_p = \frac{-P_\gamma(\omega)}{|P(j\omega)|^2}, \end{cases} \tag{33}$$

and principal axes $\frac{2}{\gamma|P(j\omega)|}$, $\frac{2\omega}{\gamma\sqrt{\omega^4+1}|P(j\omega)|}$.

As before,

$$S_\gamma(\omega) = S \setminus E_\gamma(\omega) \ \ \forall\, \omega \in [0, \infty) \tag{34}$$

and

$$S_\gamma = \bigcap_{\omega=0}^{\infty} S_\gamma(\omega). \tag{35}$$

The details of the computation are omitted.

Remark 2. We can consider the H_∞ norm with a weighting function $W(s)$ multiplied by the error transfer function in (14). In this case, replace γ in (15) by γ' where $\gamma' = \frac{\gamma}{|W(j\omega)|}$. Then, the principal axes of the axis parallel ellipse $E_\gamma(\omega)$ are subject to change by $W(j\omega)$. However, the derivation of the equations in this section remains the same.

Remark 3. If $C(s)$ is replaced by $C_\tau(s) = \frac{k_p s + k_i + k_d s^2}{s(\tau s+1)}$, then $C_\tau(s)P(s) = C(s)\frac{1}{\tau s+1}P(s)$. Since τ can be fixed a priori, we can replace $P_r(j\omega)$ and $P_i(j\omega)$ in (17) by

$$P_r'(j\omega) = \frac{P_r(j\omega) + \tau\omega^2 P_i(j\omega)}{1 + \tau^2\omega^2}$$
$$P_i'(j\omega) = \frac{P_i(j\omega) - \tau P_r(j\omega)}{1 + \tau^2\omega^2}.$$

Then, the controller design can be carried out in a similar manner.

5. EXAMPLES

We present two examples to illustrate the steps to find the set S_γ.

Example 1. Consider the second order plant and the PI controller:

$$P(s) = \frac{s-2}{s^2+4s+3}, \quad C(s) = k_p + \frac{k_i}{s}. \tag{36}$$

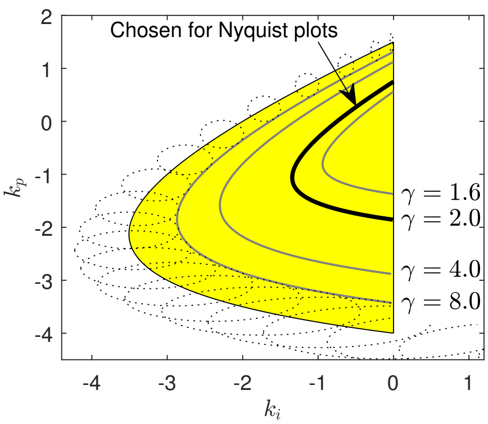

Fig. 11. S_γ for $\gamma = 1.6$, 2, 4, 8 with the stabilizing set.

The stabilizing set was first computed for the plant and the PI controller given in (36). Family of ellipses $E_\gamma(\omega)$ were drawn by sweeping over ω and S_γ were found accordingly for $\gamma = 1.6$, 2, 4 and 8. In Fig. 11 we observed that S_γ were contained in the stabilizing set S and $S_{\gamma_1} \subset S_{\gamma_2}$ if $\gamma_1 < \gamma_2$. So, S_γ for $\gamma \in [1, \infty)$ is the telescoping series of sets. If k_p, k_i were chosen from sets S_γ, the Nyquist plot must stay outside of the critical point $-1 + j0$ with the minimum distance of $1/\gamma$. We chose some boundary points in S_γ that were inside the stabilizing set S where $\gamma = 2$ and draw the Nyquist plots in Fig. 12. Each Nyquist plot was at least 0.5 away from the critical point.

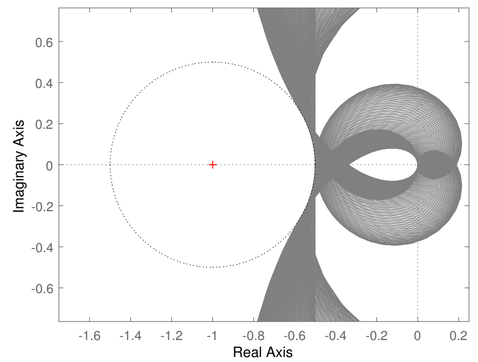

Fig. 12. Nyquist plots with k_p, k_i along the curve of $\gamma = 2$.

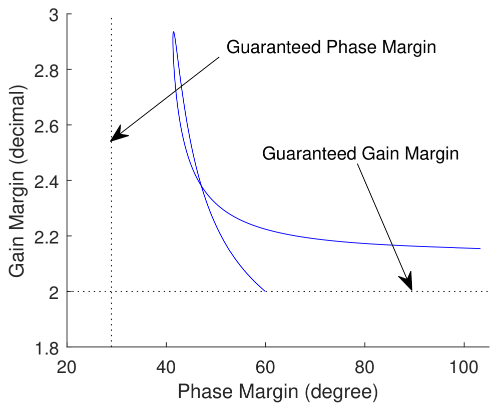

Fig. 13. Guaranteed gain and phase margin of the boundary points of S_γ for $\gamma = 2$

Following Theorem 1, the guaranteed gain margin was

$$\left[\frac{\gamma}{\gamma+1}, \quad \frac{\gamma}{\gamma-1}\right] = \left[\frac{2}{3}, \quad 2\right], \tag{37}$$

and the guaranteed phase margin ϕ was

$$\phi = 2\sin^{-1}\left(\frac{1}{2\gamma}\right) = 28.955^o \tag{38}$$

for $\gamma = 2$. Fig. 13 shows the guaranteed gain and phase margins when we choose k_p and k_i from S_γ for $\gamma = 2$. For all controllers achieving the same H_∞ norm at the boundary of S_γ, there is a trade off between gain and phase margins. When higher gain margin is desired, one should sacrifice some phase margin and vice versa. Nevertheless with the H_∞ norm we get the guaranteed gain and phase margins calculated in Eqs. (37) and (38).

Example 2. Consider a rational transfer function given in Blanchini et al. (2004) and the PID controller:

$$P(s) = \frac{10s^3 + 9s^2 + 362.4s + 36.16}{2s^5 + 2.7255s^4 + 138.4292s^3 + 156.471s^2 + 637.6472s + 360.1779} \tag{39}$$

$$C(s) = k_p + \frac{k_i}{s} + k_d s. \tag{40}$$

The stabilizing set was computed using the signature method as shown in Fig. 14. We adopted $k_d = 9$ as in Krajewski and Viaro (2012) and computed S_γ for $\gamma = 1$ in k_p, k_i plane. Fig. 15 shows the S_γ and the family of ellipses.

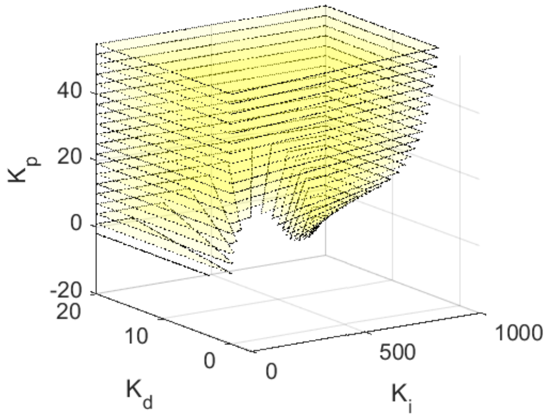

Fig. 14. The stabilizing set in k_p, k_i, k_d space using the signature method.

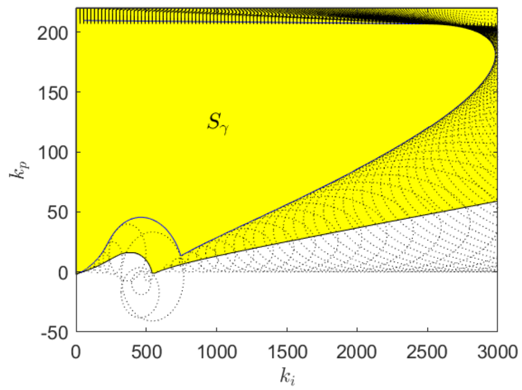

Fig. 15. S_γ and family of ellipses E_γ for $\gamma = 1$ in k_p, k_i plane with $k_d = 9$.

We observed that the stabilizing set with $k_d = 9$ was unbounded in k_p, k_i plane. However, the S_γ for $\gamma = 1$ in the same plane was bounded. For the high values of ω the major and minor axes of the ellipses grow as the centers c_1 and c_2 in (26) go away from the origin. So, we suggest that the family of ellipses be computed for high enough values of ω to get the exact set S_γ.

Clearly in this case, S_γ is not empty and the H_∞ norm condition less than $\gamma = 1$ provides very good robustness, namely $[0.5, \infty]$ gain margin and 60^o phase margin. Thus, all of the points in S_γ guarantee such good robustness. In fact, since the open loop transfer function $P(s)C(s)$ is strictly proper, the Nyquist plot of $P(j\omega)C(j\omega)$ goes to 0 as $\omega \to \infty$ and so every point in S_γ achieves the same H_∞ norm.

Time response considerations

So far we have discussed stability and robustness. However, the design of a controller should pay attention to the time response considerations. In order to demonstrate, we chose the following three design points:

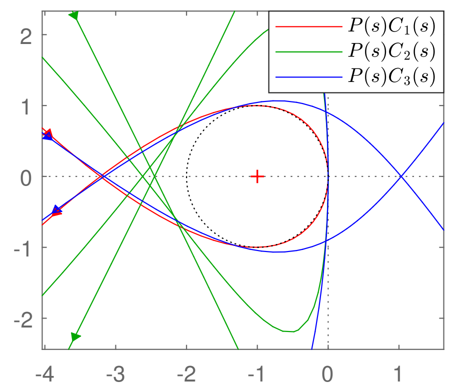

Fig. 16. Nyquist diagram for $P(s)C_1(s)$ (red), $P(s)C_2(s)$ (green) and $P(s)C_3(s)$ (blue).

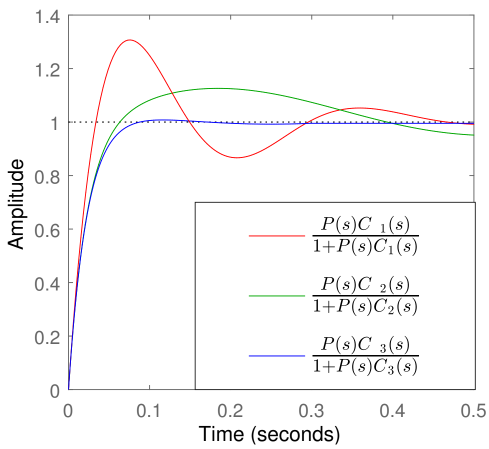

Fig. 17. Step responses for the closed loop systems of $P(s)C_1(s)$ (red), $P(s)C_2(s)$ (green) and $P(s)C_3(s)$ (blue).

$$\begin{cases} C_1(s) = 185 + \frac{2986}{s} + 9s, \\ C_2(s) = 20 + \frac{800}{s} + 9s, \\ C_3(s) = 19 + \frac{200}{s} + 9s. \end{cases} \tag{41}$$

The first point has the maximum k_i value in S_γ, the second is adopted from Krajewski and Viaro (2012) and the third is an arbitrary point from the boundary of S_γ with a relatively lower k_i value.

The Nyquist plots in Fig. 16 confirms that all three design points satisfy the robustness condition. The step responses in Fig. 17 shows that the three controller designs result in different time responses in terms of overshoot and settling time. While $C_1(s)$ and $C_2(s)$ have highest and intermediate integral gains, $C_3(s)$ provides much shorter settling time and lesser overshoot than the other two controllers do.

The integrator in the controller provided zero steady state error and we found all stabilizing controllers achieving prescribed H_∞ norm of the error transfer function. While the robustness and zero steady state error could be achieved by the proposed method, one should also consider the quality of the transient response when tuning the PID parameters within the set S_γ. Thus, the PID controller design for better transient response within the same degree of robustness is an important area of research.

6. CONCLUDING REMARKS

The results of this paper could be extended to discrete time and time-delay systems. Another important area of research is the extension of these results to multivariable systems.

REFERENCES

Ashfaque, B.S. and Tsakalis, K. (2012). Discrete-time PID controller tuning using frequency loop-shaping. *IFAC Proceedings Volumes*, 45(3), 613–618.

Bhattacharyya, S.P., Datta, A., and Keel, L.H. (2009). *Linear control theory: structure, robustness, and optimization*, volume 33. CRC press.

Blanchini, F., Lepschy, A., Miani, S., and Viaro, U. (2004). Characterization of PID and lead/lag compensators satisfying given H_∞ specifications. *IEEE Transactions on Automatic Control*, 49(5), 736–740.

Díaz-Rodríguez, I.D. and Bhattacharyya, S.P. (2016). PI controller design in the achievable gain-phase margin plane. In *Decision and Control (CDC), 2016 IEEE 55th Conference on*, 4919–4924. IEEE.

Emami, T. and Watkins, J.M. (2009). Robust performance characterization of pid controllers in the frequency domain. *WSEAS transactions on systems and control*, 4(5), 232–242.

Krajewski, W. and Viaro, U. (2012). On robust PID control for time-delay plants. In *Methods and Models in Automation and Robotics (MMAR), 2012 17th International Conference on*, 540–545. IEEE.

Tantaris, R.N., Keel, L.H., and Bhattacharyya, S.P. (2006). H_∞ design with first-order controllers. *IEEE Transactions on Automatic Control*, 51(8), 1343–1347.

Tsakalis, K.S. and Dash, S. (2013). Approximate H_∞ loop shaping in PID parameter adaptation. *International Journal of Adaptive Control and Signal Processing*, 27(1-2), 136–152.